AFRL-OSR-VA-TR-2015-0020

ENGINEERING ROBUST NATURAL NANOCOMPOSITE NETWORKS

Jeffrey Urbach
GEORGETOWN UNIVERSITY (THE)

12/16/2014
Final Report

Air Force Research Laboratory
AF Office Of Scientific Research (AFOSR)/ RTD
Arlington, Virginia 22203
Air Force Materiel Command

REPORT DOCUMENTATION PAGE

Form Approved
OMB No. 0704-0188

1. REPORT DATE *(DD-MM-YYYY)*	**2. REPORT TYPE**	**3. DATES COVERED** *(From - To)*
12/11/2014	Final Progress Report	9/1/2019–8/31/2014

4. TITLE AND SUBTITLE
Engineering Robust Nanocomposite Networks

5a. CONTRACT NUMBER

5b. GRANT NUMBER
FA-9550-10-1-0473

5c. PROGRAM ELEMENT NUMBER

6. AUTHOR(S)
Jeffrey S. Urbach

5d. PROJECT NUMBER

5e. TASK NUMBER

5f. WORK UNIT NUMBER

7. PERFORMING ORGANIZATION NAME(S) AND ADDRESS(ES)

Georgetown University
37th & O Sts.
Washington, DC 20057

8. PERFORMING ORGANIZATION REPORT NUMBER

9. SPONSORING / MONITORING AGENCY NAME(S) AND ADDRESS(ES)
AFOSR

10. SPONSOR/MONITOR'S ACRONYM(S)

11. SPONSOR/MONITOR'S REPORT NUMBER(S)

12. DISTRIBUTION / AVAILABILITY STATEMENT

Approved for Public Release

13. SUPPLEMENTARY NOTES

14. ABSTRACT

In this grant period we were able to make significant advances in our understanding of a number of issues related to the processing and properties of nanocomposite networks. We showed that a non-Brownian suspension of micron scale rods exhibits reversible shear-driven formation of disordered aggregates resulting in dramatic viscosity enhancement at low shear rates. We also developed a new technique, Boundary Stress Microscopy, to quantify the non-uniform surface stresses in sheared collagen gels. In our collaborations with other AFOSR supported research, we were able to show that native silk solutions can for fibers directly as a result of applied shear, that silk e-gels show remarkable elasticity and work hardening, and that the luminous mucous secreted by the marine worm Chaetopterus sp. behaves rheologically as a yield stress gel.

15. SUBJECT TERMS

16. SECURITY CLASSIFICATION OF:			**17. LIMITATION OF ABSTRACT**	**18. NUMBER OF PAGES**	**19a. NAME OF RESPONSIBLE PERSON**
a. REPORT	**b. ABSTRACT**	**c. THIS PAGE**			**19b. TELEPHONE NUMBER** *(include area code)*

Engineering Robust Nanocomposite Networks

Principle Investigator: Dr. Jeffrey Urbach
Institution: Georgetown University
Award: FA-9550-10-1-0473
Program Manager: Dr. Hugh C. DeLong

Abstract:

In this grant period we were able to make significant advances in our understanding of a number of issues related to the processing and properties of nanocomposite networks. We showed that a non-Brownian suspension of micron scale rods exhibits reversible shear-driven formation of disordered aggregates resulting in dramatic viscosity enhancement at low shear rates. Aggregate formation was imaged using a combined rheometer and fluorescence microscope. The size and structure of these aggregates are found to be a function of shear rate and concentration, with larger aggregates present at lower shear rates and higher concentrations. Quantitative measurements of the early-stage aggregation process were modeled by collision driven growth of porous structures which suggest that the aggregate density increases with shear rate. This result was combined with a Krieger–Dougherty type constitutive relationship and steady-state viscosity measurements to estimate the intrinsic viscosity of complex structures developed under shear. These results represent a direct, quantitative, experimental demonstration of the association between aggregation and viscosity enhancement for a rod suspension, and demonstrate a way of inferring microscopic geometric properties of a dynamic system through the combination of quantitative imaging and rheology.

We also developed a new technique, *Boundary Stress Microscopy,* to quantify the non-uniform surface stresses in sheared collagen gels. We found that local stresses exceeding average stresses by an order of magnitude, with variations over length scales much larger than the network mesh size. The strain stiffening behavior observed over a wide range of network mesh sizes can be parameterized by a single characteristic strain and associated stress, which describes both the strain stiffening regime and network yielding. The characteristic stress is approximately proportional to network density, but the peak boundary stress at both the characteristic strain and at yielding are remarkably insensitive to concentration. The form of stress propagation is central to understanding many important mechanical properties, including the ultimate strength of a material and the nature of appropriate microscopic constitutive equations.

In our collaborations with other AFOSR supported research, we were able to show that native silk solutions can for fibers directly as a result of applied shear, that silk e-gels show remarkable elasticity and work hardening, and that the luminous mucous secreted by the marine worm Chaetopterus sp. behaves rheologically as a yield stress gel.

Accomplishments

Quantification of shear-induced aggregation of rod suspensions:

Approach: We have developed a well-controlled model system for studying the effects of shear flow on fiber suspension structure and rheology. Specifically, we have been able to produce suspensions of fluorescent SU-8 microrods by modifying published protocols to include fluorescein salt during the processing. The as-made rod suspension is purified by filtering and, if desired, glycerol density gradient centrifugation in order to produce a relatively uniform length distribution (Fig. 1). The resulting rods, dispersed in either glycerol/ethylene glycol or in MnCl2-water solutions, provide a density-matched model systems for studying both weakly-Brownian and non-Brownian suspensions that occur during the production of fiber-reinforced composites.

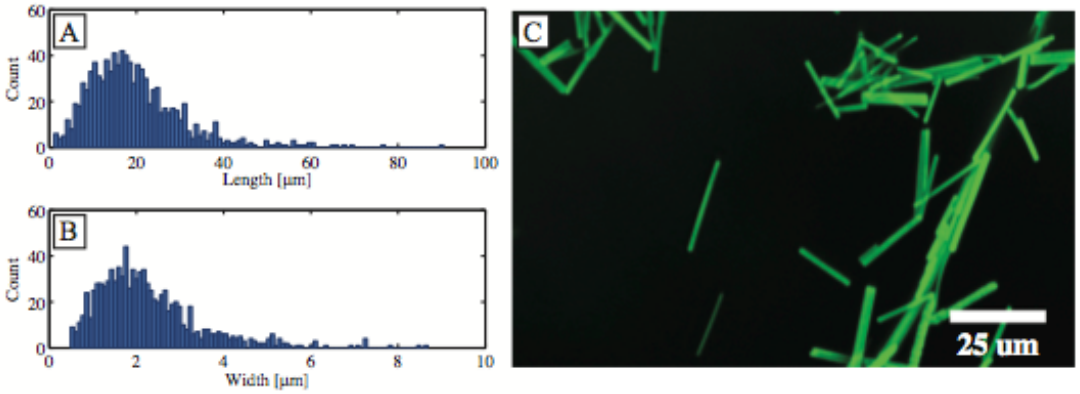

Figure 1: Representative (A) length, and (B) width distribution of polydisperse SU-8 microrods (before density gradient centrifugation) depicted in (C). Mean length is 19.6 μ*m* with a standard deviation of 11.1 μ*m*. Mean diameter is 2.3 μ*m* with a standard deviation of 1.2 μ*m*

Results: We have discovered that a non-Brownian fiber suspension made up of the microrods dispersed in a density-matched Glycerol-Glycol solvent forms roughly spherical aggregates when subject to controlled shear, and that the formation and breakup of these aggregates is fully reversible. We have used our coupled Rheometer-Microscope instrument to visualize the growth of the aggregates starting from a fully dispersed state (Fig. 2).

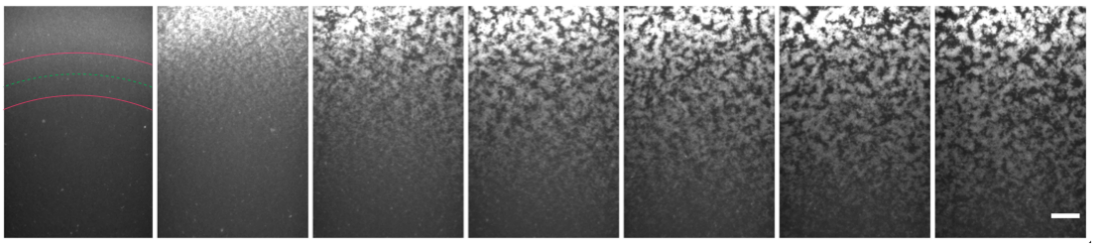

Figure 2: The aggregation of an φ = 0.07 SU-8 microrod suspension subject to a steady shear (1.5 1/s edge shear rate), starting from a dispersed state. From left to right, the images are taken at 0, 50, 100,

150, 200, 250, and 300 seconds from the start of shearing. The flow direction is tangential with respect to a circle whose center is located below the displayed images, slightly out of frame. The region considered for analysis is highlighted in the first image of the montage. The scale bar represents 1mm.

Using the normalized intensity autocorrelation function, calculated along arcs of constant shear rate, we can extract an aggregate length scale that increases with time (Fig. 3A), eventually saturating at a size that decreases with increasing shear rate (3B). The length scale versus time for different shear rates can be converted to length versus integrated strain, showing an initial growth that is independent of shear rate (C,D). This general behavior has been observed in a wide range of fiber suspensions, but these results provide the first quantification with sufficient precision to validate physical models for aggregate formation and breakup.

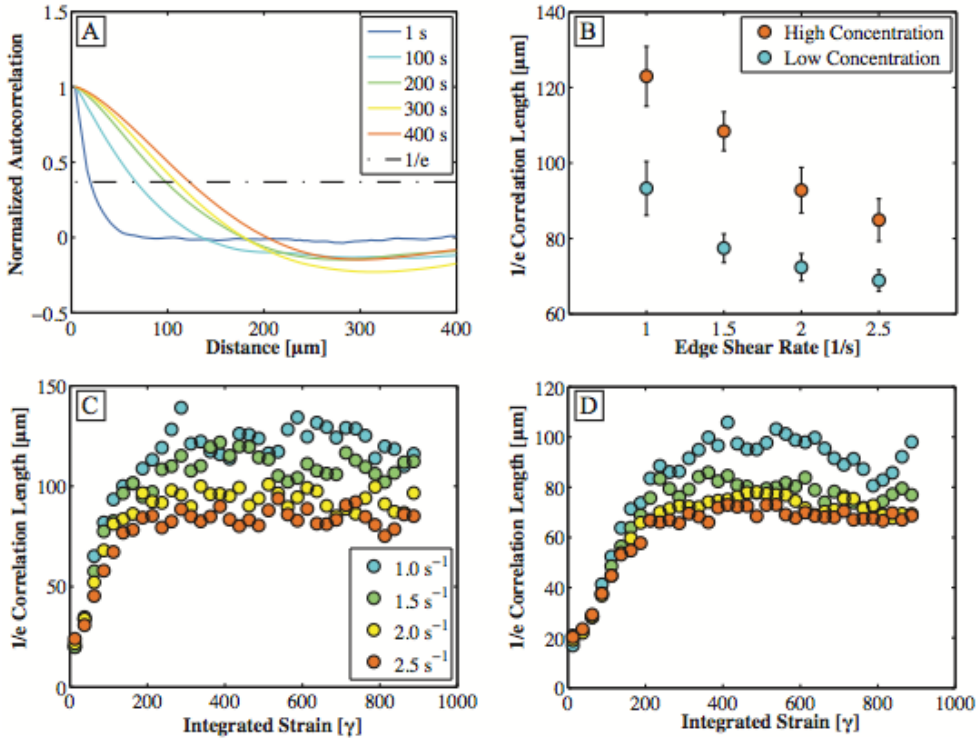

Figure 3: (a) Intensity autocorrelation at different times after the start of shearing for φ = 0.07 concentration suspensions, with an applied shear rate of 1 1/s. The aggregate length scale is defined to be the length at which the normalized autocorrelation function crosses 1/e. (b) The steady state aggregate length scale decreases with increasing shear rate. (c, d) Aggregate length scale increases as shear-induced structures form in (c) φ = 0.07 and (d) φ = 0.04 SU-8 microrod solutions. Within a concentration, the aggregation rates appear nearly identical when normalized by integrated strain. Higher concentrations, however, appear to aggregate faster than lower concentrations consistent with shear-driven collision based processes.

In collaboration with Aparna Baskaran at Brandeis, we have begun testing models of the aggregation process. Fig. 4A shows an example of a fit to an exponential growth model, appropriate for sheared suspensions of non-Brownian attractive particles. The model does a reasonably good job of describing the growth regime, and the only free parameter is the density of the rod aggregates. Fig. 4B shows the aggregate density extracted from the fits as a function of shear rate, for two different concentrations. We find that the aggregate density increases with shear rate,

presumably because the increased shear stresses more effectively compact the aggregate. This effect can then be used to explain the steady state thixotropic behavior of the rod suspensions at modest concentrations, using a fit to the Krieger-Dougherty equation that describes viscosity enhancement due to the presence of suspended particles (4C). The model fails at high concentrations, however (4D) likely because the aggregates form a percolated connected network (4D, inset), resulting in gel-like behavior.

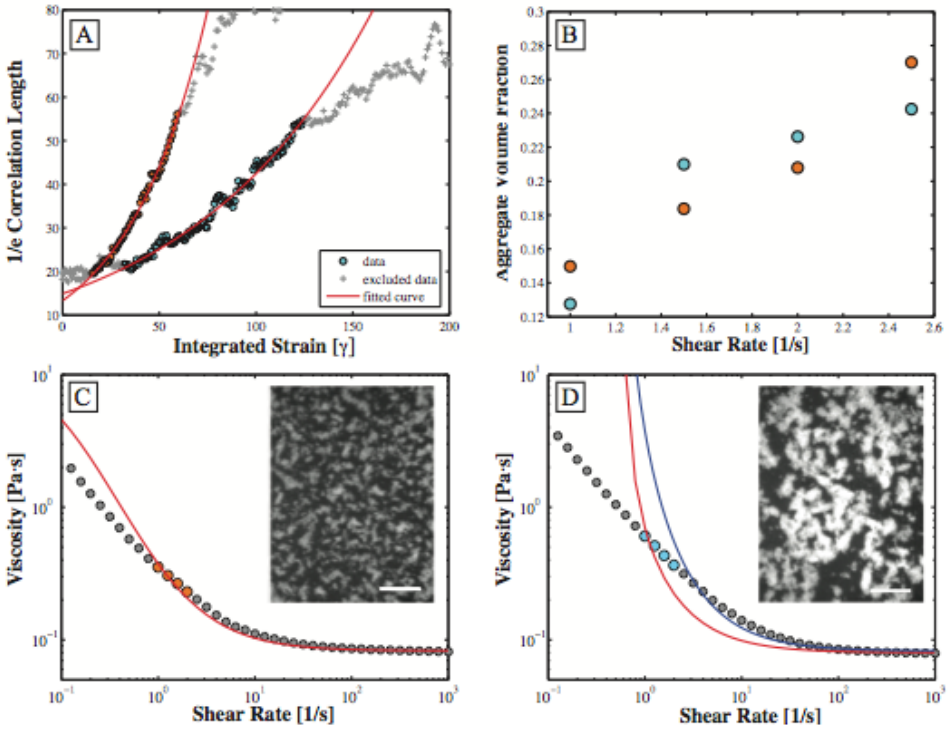

Figure 4: The early stage aggregation curves (A) closely follow the aggregation model in the scaling region. Representative data is shown for φ = 0.07 (turquoise) and φ = 0.04 (orange) at $\dot{\gamma}$ = 1 1/s. The fits reveal an aggregate density that increases with shear rate (B). Krieger-Dougherty (KD) derived fits that take into account increasing aggregate density with shear rate work well for lower concentrations (C), but not high concentrations (D), consistent with the system evolving into a gel-like state (D,inset) rather than a fluid-like state (C, inset).

We have also formed aggregates in our Confocal-Rheometer and have observed detailed surface structure that lacks any obvious ordering (Figure 5). Extracting this surface structure will allow us to predict flow fields around aggregates using finite element methods. These flow fields transmit stresses responsible for viscosity enhancement and aggregate breakup. This work was reported in an article published in *Soft Matter* in 2014.

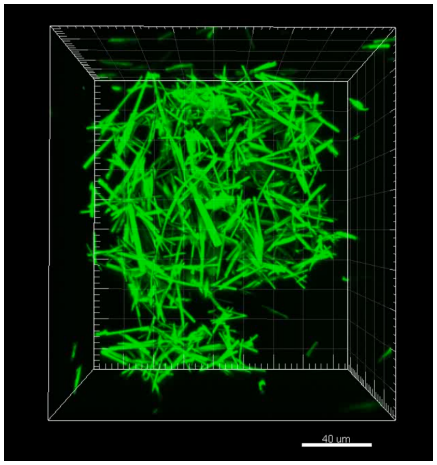

Figure 5: The 3D surface structure of an SU-8 microrod aggregate formed under shear, and captured using a confocal microscope, appears highly disordered. In movies, structures such as this one appear to dramatically disrupt the surrounding flow field.

Torsional resistance determines ordering of rod aggregates:

Approach: We have developed mesoscale simulations using the LAMMPS molecular dynamics simulator and its implementation of dissipative particle dynamics (DPD), and successfully employed the AFOSR HPC resources for large scale parallel computation. A model fiber system's viscosity, stresses, fluid velocity field, and relevant forces can be determined by simulating its evolution in shear flow. We can control the fluid viscosity (and therefore the importance of Brownian motion) and incorporate a variety of fiber-fiber interactions with combinations of standard pairwise forces. The study of simulated aggregation facilitates the quantification of force competition and timescales and allows us to explore the parameter space relevant for a wide range of natural fiber systems.

Results: Figure 6 shows a rendering of the simulation environment. The box represents the simulated domain, which is periodic in both horizontal dimensions. The shear is in the vertical direction, which is bounded by rough walls. The approximately 10^9 fluid particles are rendered only in the back half, so that the randomly oriented rigid rods can be observed.

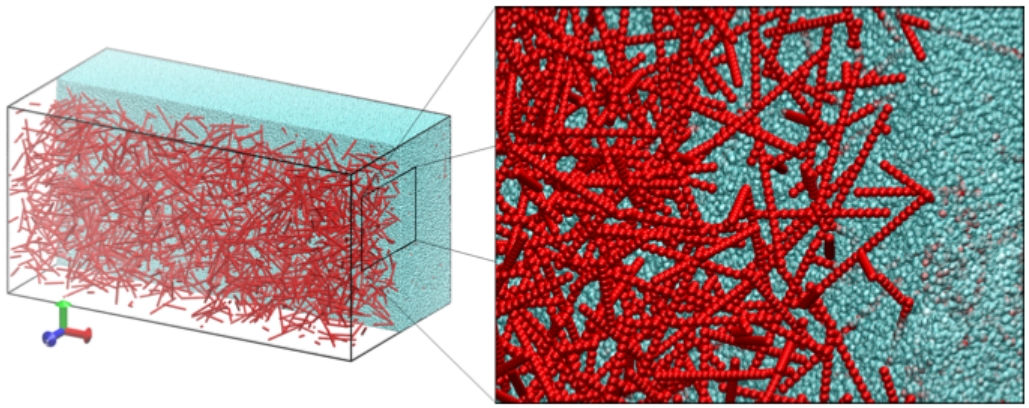

Figure 6: Model system with rigid rod-like particles, composed of strings of spheres, shown in red, and DPD fluid particles rendered only in the back half of the simulation volume. The initial condition (before shearing in the x/Red direction) is random in both position and orientation.

Shortly after the start of the shearing process, the rods align in the velocity direction, as expected for high aspect ratio particles in a strong shear, and bundle in the presence of attractive interactions (Fig. 7, left). We have found that bundling and proto-fiber formation is quite generic, while disordered aggregates like those seen in our experiments are not. However, we discovered that the addition of torsional stiffness to the rod-rod contacts suppresses the bundling (center), and if it strong enough, produces fully disordered aggregates (right).

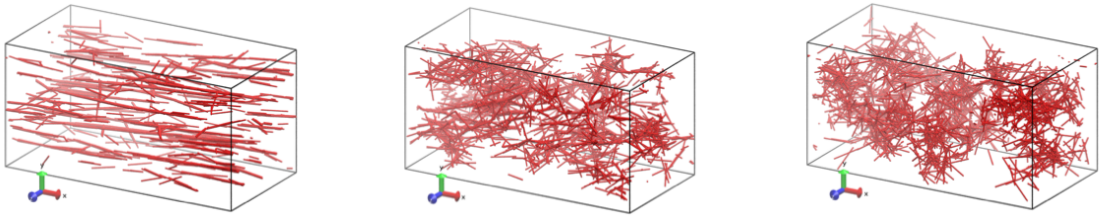

Figure 7: Simulations of shear induced rod aggregation. After the application of steady shear, rods with attractive interactions form aligned bundles. The addition of moderate torsional stiffness to rod-rod contacts results in partially disordered aggregates, and high torsional stiffness produces completely disordered aggregates, similar to those seen in the experiments.

We have quantified this behavior with measures of the average number of particles in the aggregated phase, average volume enclosed by the aggregates, and the degree of orientational ordered of the aggregates. We also have measured the viscosity enhancement that accompanies the aggregation process, and are testing the model developed in the experimental work. We are completing the final phases of this analysis and anticipate submitting a manuscript in the Spring of 2015.

Stress Heterogeneity in Sheared Collagen Networks:

Approach: We developed a new technique which we have termed *Boundary Stress Microscopy* to directly image heterogeneous stress propagation in a disordered rigid polymer networks. In our initial studies, we investigated the nonlinear rheological

properties of branched type-1 collagen gels, a material that undergoes substantial strain stiffening, common to many disordered semi-flexible or stiff polymer networks.

Boundary Stress Microscopy is an extension of the traction force microscopy approach for the study of cellular biophysics. Briefly, fibrillar collagen networks are polymerized *in situ* between a polyacrylamide gel and the rheometer tool. The motion of fiduciary fluorescent beads in the polyacrylamide gels is imaged by confocal microscopy, allowing for measurement of the deformation of the collagen/polyacrylamide boundary, which can be converted to the three-dimensional local surface stress (shear stress and normal force) using established techniques.

Results: We have performed measurements over a wide range of collagen concentrations, representing collagen fibril areal densities that range over about a factor of 30. The *local* stress-strain curves, determined directly from the average boundary stress calculated from the polyacrylamide deformations, are shown in Fig. 8A. Both the local (measured from the boundary stresses) and global (measured by the rheometer, not shown) stress-strain show similar behavior at all concentrations: a nonlinear increase in stiffness, followed by a roughly linear regime of high stiffness, followed by a flattening and eventual decrease in stress (not shown), signaling the onset of network integrity loss. Thus the instantaneous stiffness, or dynamic modulus, increases rapidly, then saturates, and finally begins to decrease. We use the locally applied strain at maximum curvature found by numerically differentiating the smoothed dynamic modulus curves, as a precise, objective measure for systematically comparing the behavior from gels of different concentrations. Fig. 8B shows the measured local stress and the local. The curves show a near complete data collapse, except at the highest concentration, confirming the qualitative observation that the strain stiffening curves show universal behavior.

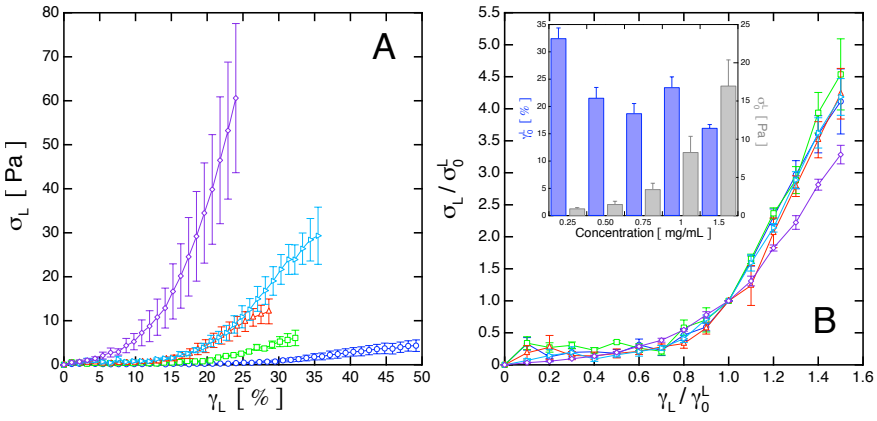

Figure 8: A) Local stress-strain curves for a range of collagen concentrations. B) Rescaling by the stress and strain values at maximum curvature produces a universal response curve for all concentrations. Scaling parameters shown in the inset. Error bars represent standard error from 3-4 trials.

The reference strains shown in the insets are roughly independent of concentration (except at the lowest concentration), consistent with results in the literature identifying a characteristic strain as the point where the dynamic modulus exceeds

the low strain value by a fixed percentage. The values of the characteristic stress are strongly dependent on concentration, varying by approximately 30 from the lowest concentration to the highest. Much of this variation can be accounted for by the increase in network density: The stress times the square of the mesh size, representing the average force per fiber, is roughly constant, suggesting that the microscopic, fiber-level origins of the strain stiffening are similar at all concentrations.

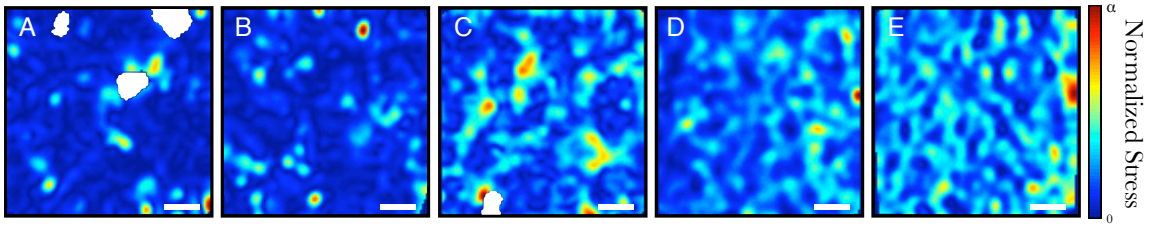

Figure 9: Normalized boundary stresses in collagen networks with the same concentrations as in the top panel, at 1.5 times the characteristic strain. Each map is normalized by the peak stress. Scale bar = 25 μm.

Figure 9 shows representative normalized stress maps at each of the concentrations shown in Fig. 8 at 150% of the reference strain, showing that stresses are heterogeneously distributed over length scales much larger than the network mesh size. We observe local stresses as much as an order of magnitude larger than the average stresses, and find that quantitative measures of the heterogeneity increase with strain stiffening. We also found that the peak stresses at the yield (the stress necessary to tear the network) are remarkably insensitive to concentration. Our results are consistent with a stiffening and yielding response that is determined by a subset of collagen fibers that reorient and stretch in response to applied shear. This work is described in a manuscript currently under review in *PLoS One*.

Interactions:

Silk e-Gel Rheology (Kaplan, Tufts)

In a continuing collaboration with the Tufts university silk group lead by Prof. David Kaplan, we have explored the properties of reconstituted silk gels through a stepwise processing procedure that provides direct insights into gel formation of structure through rheological measurements.

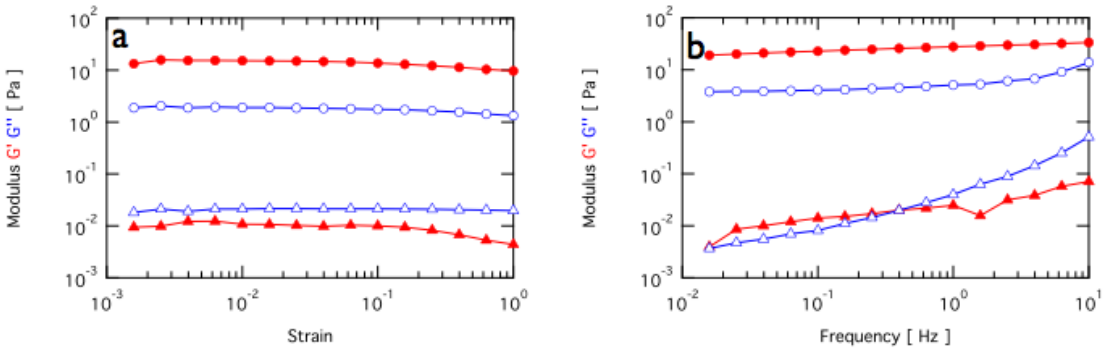

Figure 10: Silk e-gel rheology G' (closed symbols) and G'' (open symbols) of silk fibroin solution (triangles) and e-gel (circles) through a linear viscoelastic (a) strain sweep at f=0.5 Hz and (b) frequency sweep at 0.01 reveal that e-gelation transforms the mildly viscoelastic solution into an elastic gel with dynamic moduli that are largely strain and frequency independent over a wide range.

We now have a robust and systematic procedure for the creation of silk e-gels that ensures that the electro-gelled material is free of bubbles, providing a pristine gel that can be measured and manipulated. We are now able to directly compare the mechanical response of the reconstituted silk solution and the pristine e-gels. In Figure 10, the linear oscillatory rheology is shown for the protein solution and the e-gel. As expected, the solution has a predominantly fluid-like behavior over the entire range of strains, exhibiting the signatures of a weak viscolastic fluid. However, we find that for the e-gel, the elastic modulus G' is more than three orders of magnitude greater than the solution, with the loss tangent -- a measure of the ratio of the elastic to viscous components -- $\tan(\delta) \sim 0.1$ indicative of an elastic solid. Moreover, over a broad range of frequencies, at a fixed strain amplitude, (Fig. 10 b), the e-gel moduli exhibit a weak power-law increase, indicative of a glassy or gel-like response often observed in a broad class of disordered soft solids.

We have quantified the remarkable elastic properties of the e-gels with creep and stress relaxation measurements, and found that under some conditions they behave elastically to strains of over 1000%. To distinguish the elastic and plastic regimes of the e-gel network, we performed strain recovery tests on the e-gels (Figure 11).

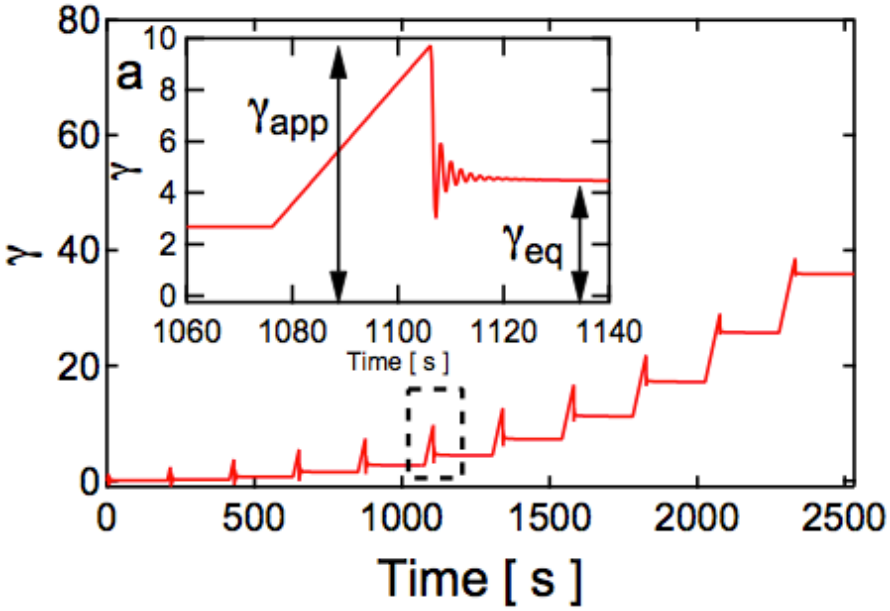

Figure 11: A representative strain history for an e-gel undergoing a strain recovery test. Each gel is subject to stepwise increasing applied rotational strains up to a maximum and allowed to relax back to an equilibrium position after each strain; the inset highlights the interval in the dashed box. The new equilibrium strain position is recorded and a modulus measurement is made before the next strain cycle.

We apply a strain γ_{app}, on the e-gel at a rate of 1.0 s^{-1} and let it return to an equilibrium strain position, recovering a certain percentage of the original applied strain (Fig. 12, open symbols). The modulus is measured at this resting position with a small strain amplitude oscillatory test (Fig. 12, closed symbols), and the gels are strained again by an increasing amount. The e-gel recovery can be separated into two regimes. For $\gamma_{app} < 5$, the e-gel acts elastically with a strain recovery greater than 75% and $G'/G_0 \sim 1$. For $\gamma_{app} > 5$, the significant decrease in strain recovery indicates a plastic deformation and is accompanied by the increase in G'/G_0. The fact the modulus ratio compared to the undeformed material rises implies that the material is transitioning into a state with another microstructure that has a modulus that is up to 4 times greater. We are currently investigating the microscopic origins of this strain-induced transformation.

This work was reported in an article in press in *Soft Matter*.

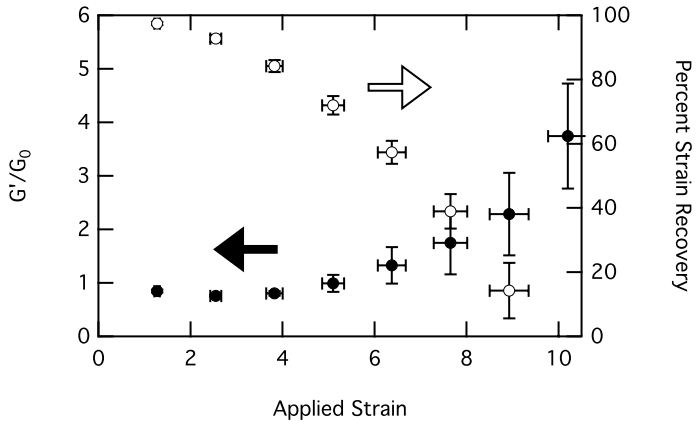

Figure 12: Results for the strain recovery test (Fig. 11). Error bars in the x-direction represent a range of applied strains amongst different trials, not an uncertainty. Percent strain recovery (open symbols) as a function of applied strain shows that the e-gel is able to recover significantly from strains that would cause yielding in most biopolymers. Upon return to the new equilibrium strain position, the modulus (closed symbols), G', stays consistent with the zero-shear modulus, until a significantly large strain. This increase in modulus coincides with the decreasing recovery of the e-gel system.

Shear-induced fibril formation in native silk Dope: (Vollrath and Holland, Oxford)

In collaboration with the Oxford silk group lead by Prof. Fritz Vollrath and Dr. Chris Holland, we are investigating the formation of silk fibers in native silk dope. This work is providing new directions for investigating the biomechanics of fiber formation in silk. Through the application of bulk shear coupled with direct, real-space visualization, we are, for the first time, quantifying the role of simple shear in the production of silk fibers.

The combination of confocal microscopy with rheology provides unique insights into the direct connection between applied shear and the fibrillation of silk proteins in as close to *in vivo* conditions as currently possible. Our measurements demonstrate that unlike typical synthetic polymers, native silk proteins are able to *spontaneously* self-assemble, fibrillate and develop hierarchical structures upon controlled shearing, and that the shear induced fibrilogenesis is accompanied by

dramatic changes in the rheological response. These observations suggest that natural spinning may be far less complex than previously assumed. This work was reported in an article published in *Soft Matter* in 2012.

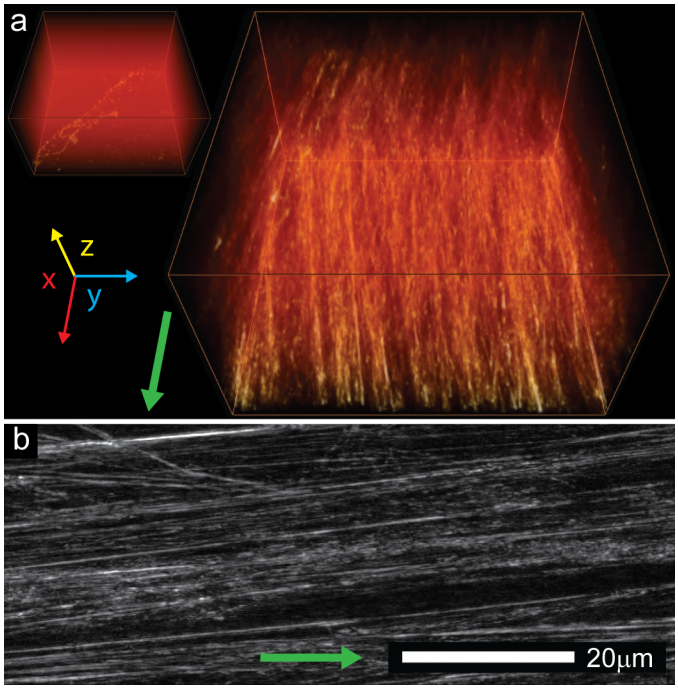

Figure 13: Shear induced silk fibrillation visualized by confocal rheology. a) 3-dimensional image of silk dope before (top left, inset) and after shear (bottom right). Bounding boxes are z stacks taken at 0.1μm intervals of size 77.5 x 77.5 x 38 μm (x,y,z). b) Detail of fibrillation in a representative horizontal slice (x,y) of the sample taken at 5 μm above the lower coverslip. Green arrows represent the direction of shear.

Rheology of Luminous Mucous Secreted by the Marine Worm Chaetopterus sp. (Deheyn, Scripps)

Mechanical testing of secreted mucus was performed using a stress-controlled rheometer (Anton Parr GmbH MCR-301). The tool geometry was a peltier temperature-controlled, 50-mm diameter plate-plate configuration. Oscillatory measurements were performed to determine the viscoelastic modulus as a function of strain amplitude and oscillation frequency. To determine the linear modulus, the oscillation frequency was fixed at 6.2 rad s^{-1}, while the strain amplitude was increased logarithmically from g p 0.1% to 100%. The frequency response was determined by fixing the strain amplitude at 1.0% and logarithmically varying the oscillation frequency from 0.32 to 62.8 rad s^{-1}. Flow curves (viscosity vs. shear rate) were measured with the same tool geometry through a logarithmic variation in the applied strain rate from 0.01 to 100 s^{-1}.

When subjected to a low-amplitude oscillatory shear strain, unfiltered raw mucus exhibited a viscoelastic response with a storage modulus G′ greater than the loss

modulus G′′, indicating that the mucus is an elastic gel. Under continuous shear conditions, the mucus flowed with a viscosity that decreased as the shear rate increased. The observed shear thinning behavior is indicative of a yield stress gel. We observed that the functional form of the mucus flow curves were well described by a power law characteristic of a yield stress gel, independent of the additives or filtration history (Fig. 14). The exception comes from the addition of H2O2 that produced a large (≈500X) increase in viscosity, uniform across all shear rates tested (Fig. 14).

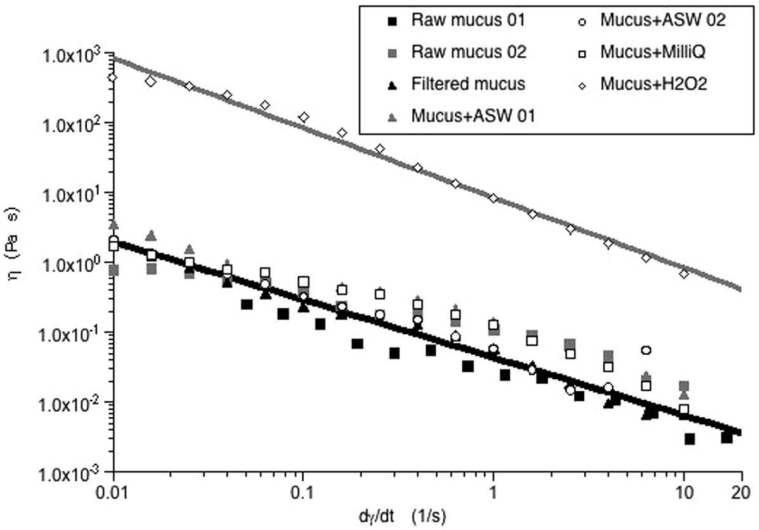

Figure 14: Change in viscosity with increasing shear rate in mucus when untreated (raw), filtered, diluted (v : v) with artificial seawater (ASW) or MilliQ water, and treated (v : v) with 30% hydrogen peroxide (H2O2).

This work was reported in an article published in Physiological and Biochemical Zoology in 2013.

Publications:

Four-dimensional structural dynamics of sheared collagen networks, Arevalo, Richard C., Urbach J. S., and Blair Daniel L. , Chaos: An Interdisciplinary Journal of Nonlinear Science, 2011, Volume 21, Issue 4, p.041102, (2011).

Direct visualization of shear dependent silk fibrillogenesis, Holland, C., Urbach J. S., and Blair D. L. , Soft Matter, 2012, Volume 8, Issue 9, p.2590, (2012).

Optical and Physicochemical Characterization of the Luminous Mucous Secreted by the Marine Worm Chaetopterus sp., Deheyn, Dimitri D., Enzor Laura A., Dubowitz Andrew, Urbach J. S., and Blair Daniel , Physiological and Biochemical Zoology, 11/2013, Volume 86, Issue 6, p.702 - 705, (2013).

Shear-Driven Aggregation of SU-8 Microrods in Suspension, P. Kumar, D. Gold, D. L. Blair, A. Baskaran, and J. S. Urbach, Soft Matter, **10:**6514–6519, (2014).

Rheology of Reconstituted Silk Fibroin Protein Gels: The Epitome of Extreme Mechanics. A. P. Tabatabai, D. L. Kaplan, D. L. Blair, Soft Matter, in Press (2014).